CORROSION SCIENCE AND TECHNOLOGY, Vol.31, No.2(2002), pp.137~142

Effect of Alloying Elements for Low-Alloy Weathering Steels for Structures in Marine/Coastal Atmosphere

Toshiaki Kodama and Toshiyasu Nishimura

National Institute for Materials Science
1-2-1, Sengen, Tsukuba, 305-0047 Japan

Low-alloy weathering show poor performance in environments where airborne salinity is high. Recent research on rust and weathering steels has been focused on the rusting mechanism in the presence of chloride and the development of new steels that are resistant in marine/coastal environments. The paper focuses on 1) crystal structure of iron rust in high salinity, 2) electrochemical reaction of rust and its catalytic properties in chloride media, 3) protective nature of rust of weathering steels, 4) thermochemical aspect of rusting in chloride environments,.

Keywords *: weathering steels, marinelcoastal almosphere, rusting mechanism, chloride environments*

1. Introduction

In the earlier work on weathering steel, its corrosion performance was discussed in relation to atmospheric pollutant SOx. However, current concern over usage of weathering steel components is in the coastal environment, at least in Japan. Long-term exposure results are expressed as $\Delta W = At^N$, where ΔW, t and A are mass loss by corrosion, time and a constant. The exponent value of N is the measure for rust stabilization and is smaller than unity when rust stabilizes. Conventional weathering steels shows $N < 0.5$ in a SOx-polluted atmosphere, whereas it sometimes gives a value greater than unity in sea-salt laden atmosphere leading to catastrophic corrosion. In such an environment, conventional weathering does not function effectively. Weathering steels have proven records of corrosion resistance against SOx and thus there is an urgent demand to enhance their resistance against chloride corrosion in a coastal environment for applications as infrastructure components.

Long-term atmospheric exposure test over 1981-1990 was carried out under the coordination of Public Works Research Institute (PWRI) by exposing test pieces on 41 bridges in Japan.[1] The results indicated clearly that the most influential factor was the sea- salt particles and that the effects of sulfur dioxide and time of wetness were minor in Japanese atmosphere. The following guidelines for usage of uncoated weathering steel for bridges was proposed: (1) Uncoated weathering steel can be used in the area where airborne salinity level is lower than 0.05 mdd in air: (2) The tolerated zone depends on the distance from shoreline and locality (Zone map is shown by PWRI). In the US, the Federal High Way Authority (FHWA) issued a guideline that uncoated weathering steel might be when chloride level as $Cl^-$is lower than 0.5 mg/ $100cm^2$/day.[2] In Japan, the use of anti-freezing salt spray is still not very widespread and this is believed to be avoided by adequate drain system design and length adjuster for steel bridges.[1]

2. Experimental

The sample materials were low alloy steels that contained 1-3 mass % of Co or Ni, 0.8% Al, or 1 mass % of W in carbon steel (JIS-SM : 0.05C - 0.3Si - 0.7Mn - 0.01 P - 0.003S - 0.03Al- 0.003N - 0.002O - Fe).

Laboratory-scale simulation procedure of atmospheric corrosion is as follows: (a) Wetting of mild steel surface by a droplet of salt solutions of a volume 20 μL / cm^2; (b) storing the sample in a cabinet maintained at a constant temperature and humidity conditions of 25℃ and RH 60% for 12 hours; (c) rinsing the steel surface with deionized water for avoiding the accumulation of excessive salt.[3, 4] The processes consisting of wetting, drying and rinsing were repeated for a number of cycles. Four types of saltwater ranging from 0.005 to 5 % NaCl were used for wetting metal surface in a e simulation of adherent saline particles. Continuous phase change in rust was observed using a specially designed cell attached to an x-ray diffraction (XRD) device, which allowed an *in-situ* measurement

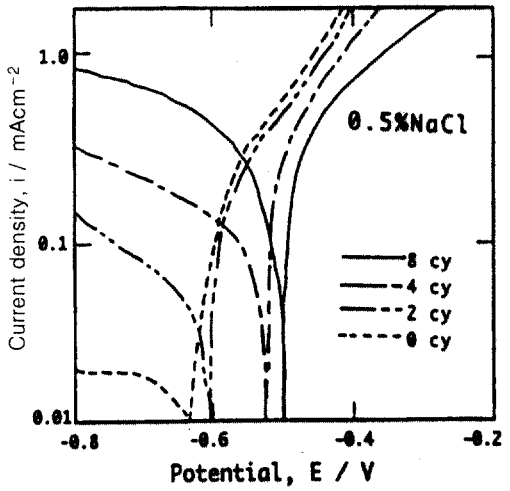

Fig. 1. Polarization curves of rusted steels processed by wet/dry/rinse cycle. Cathodic current markedly increases with increase in number of corrosion cycles.

of corroded surface in humidified atmosphere. In parallel with the corrosion tests, electrochemical measurements were carried out by means of potentiostatic polarization.

After the corrosion test, the rust was investigated by electron probe X-ray microanalysis (EPMA), X-ray photoelectron spectroscopy (XPS), transmission electron microscopy (TEM), and other analytical procedures. The EPMA was carried out using a JEOL JXA-8600MX, with an acceleration voltage of 15 kV, an irradiation current of 1 x 10^{-7} A, and a beam diameter of 1 um. XPS was performed using the SSX-100 (SSI), an X-ray source of Al Ka beam, having a beam diameter of 600 um. For the TEM observations, rust was collected from the specimen and crushed for about 10 min in an agate mortar, then it was fixed on a Cu mesh with carbon vapor deposits. The observations were made with a Philip CM200. EDXS analysis was carried out using PV9900 (EDAX).

3. Results and discussion

3.1 Rust formation on steel in chloride media by laboratory cyclic test

Figure 1 shows electrochemical polarization curves for rusted steels after wet-and-dry cyclic test. Potentiostatic polarization curves were obtained in a 0.5% NaCl solution under both aerated and unaerated conditions. Cathodic current increases remarkably with an increase in number of wet/dry cycles. The increase is attributed to the electrochemical reduction of rust rather than dissolved oxygen reduction or hydrogen evolution because of the reasons as follows: 1) Cathodic current increases with an increase in cycle number, or the amount of rust on metal: 2) Cathodic current starts to flow at potentials much nobler than that of hydrogen evolution. Also it should be noted that such an increase in cathodic current occurs only for rust formed in chloride media and only for rusts in contact with steel. Isolated rust shows no such effect on the cathodic reduction. Above phenomena suggest that rust formed in chloride media shows specific reactivity in its reduction process, which in turn accelerates anodic reaction of substrate metal.

3.2 Stability of rust on carbon steel in chloride media

Using a technique called *in-situ* XRD structural change of rust was followed on actually corroding surface of steel in a cycle of wet-and-dry process. Characteristic nature of XRD under high salinity was the occurrence of β

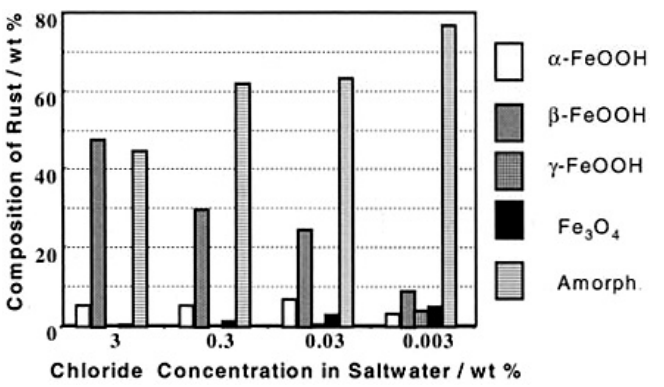

Fig. 2. XRD analysis of rust on carbon steel in chloride media. Eight cycles of dry/wet test.

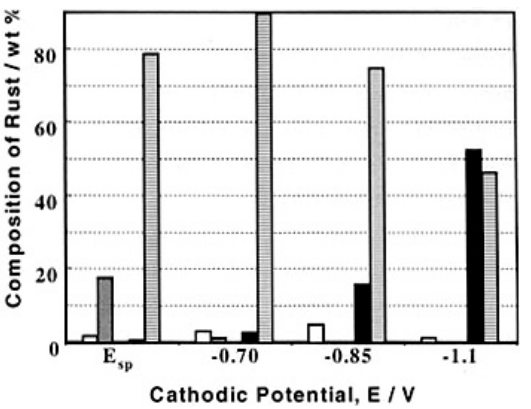

Fig. 3. Structural change of rust after cathodic reduction at various potentials Original rust was prempared in 0.3% NaCl spray/dry test.

-FeOOH which otherwise does not occur. Also detected was Green rust I (GRI), which is the mixed ferric and ferrous product occurring as an intermediate product to β-FeOOH.[4] Figure 2 and 3 show quantitative structural analyses of rust by means of XRD (*ex-situ* method in this case). The procedure for the quantitative analysis of rust composition is as follows. X-ray peak intensities of individual components (e.g. Fe_3O_4 or β-FeOOH) were determined relatively to that of CaF_2 using iron oxide/hydroxide-CaF_2 mixtures. In the actual analysis of rust, pulverized rust mixed with fixed amount of CaF2 was subjected to XRD analysis, in which quantitative determination is carried out by multiplying predetermined relative intensity factors. Undetermined portion of rust by XRD is classified into amorphous product.

Figure 2 shows the composition of rust on mild steel plotted as a function of chloride concentration in wetting media (salt fog). Obviously, β-FeOOH is predominant among crystalline products and increases with increasing chloride concentration in the corrosive media. Figure 3 shows phase transition following cathodic reduction. The original composition corresponds to that of 0.3 % Cl^- in Figure.2 It is seen from Figure. 3 that β-FeOOH is reduced to amorphous products at potentials close to spontaneous potential and to Fe_3O_4 at less noble potentials. The catalytic nature of corrosion acceleration by saltwater exists in the formation of β-FeOOH and its readiness to the reduction to amorphous, ferrous products in wet condition, which in turn accelerates anodic dissolution of substrate steel.

3.4 Redox characteristics of rust

As might be anticipated from the E-pH diagram, FeOOH rust would be eventually reduced and converted to Fe_3O_4 or Fe(II)Fe(III)-products. It was already known in the 1960s[5-7] that intense reduction current is observed for the rusted iron and that this reduction current arises from the reduction reaction of FeOOH. In response to the rust reduction, iron dissolution would proceed as the anodic reaction to form a self- catalytic cycle. In wet condition iron corrodes to form magnetite via following electrochemical reactions:

$$Fe \longrightarrow Fe^{2+} + 2\ e^-$$

$$3\ Fe^{2+} + 4\ H_2O \longrightarrow Fe_3O_4 + 8\ H^+ + 2\ e^-$$ anode reactions

and

$$3\ FeOOH + H^+ \longrightarrow Fe_3O_4 + 2\ H_2O + e^-$$ cathode reaction

in which Fe_3O_4 is assumed to represent any intermediate products containing both Fe(II) and Fe(III). In a dry period , Fe_3O_4 and other low order oxides are air oxidized to be converted to FeOOH :

$$3\ Fe_3O_4 + 3/4\ O_2 + 9/2\ H_2O \longrightarrow 9FeOOH$$

As for the redox cycle there are several mechanisms proposed. In our observation it was amorphous product, which is in agreement with Suzuki et al. Common aspect in the cycle analysis was the fact that it was γ- or β -FeOOH and not α-FeOOH that is readily reduced by the cathodic reaction. This is understandable with reference to thermodynamics and also from the fact that both γ -FeOOH and Fe_3O_4 have the closest packed structure.

3.3 Alloying elements in weathering steels

Okada et al.[8] examined rust layer formed on weathering steel under by polarized-light microscopy, EPMA and other instrumental analyses and concluded that the rust film was composed of outer FeOOH layer and dense amorphous inner layer with enriched Cu, Cr and P. These layers are distinguishable because the inner layer is extinguishes itself under crossed- Nicol prism condition, while the outer layer does not. The shielding effect by the dense inner rust layer was the key for the corrosion inhibition. Effects of alloying with Cu and P were also confirmed by means of synthetic rust prepared by colloid chemistry and also by the oxidation of $Fe(OH)_2$, in which it was demonstrated that alloying with Cu and P would promote compactness of the rust layer as well as FeOOH crystallite refinement and vitrification. All the above, as well as further experimental results acquired later, supported the essential validity of the model proposed by Okada et al.[8] Recently, Misawa and collaborators[9,10] examined rust layer deposited over weathering steel after a quarter of a century of exposure period and proposed a new model

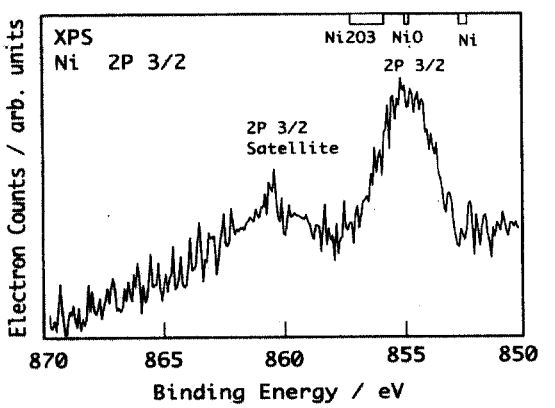

Fig. 4. XPS analysis of the rust on Ni-bearing steel. Ni in the rust in the bivalent state (Ni(II)).

for stable rust consisting of outer γ-FeOOH layer and inner α-FeOOH layer. The latter contained a few % of Cr to form compact α-$(Fe_{1-x}Cr_x)OOH$ as the major constituent of the stable rust. This evidence is seemingly contradictory to Okada's model since α-FeOOH is optically unisotropic giving no extinction under crossed Nicol prism condition. They suggested that the inner layer α-FeOOH crystallites are fine enough to be optically inactive.

Influence of Ni alloying on weathering performance of steel was discussed in Larrabee's classical work.[11] Considering the fact that the protectiveness by Ni alloying become apparent only at a higher level of Ni addition than several %, the effectiveness of Ni does not seem to be remarkable compared with other alloying elements. Nevertheless Ni is now accepted as one of the major alloying elements for weathering steels particularly for a coastal atmosphere.

3.3.1 Effect of Ni and Co addition

The rust on the surface of specimens of Co and Ni-bearing steels was analyzed after 20 times of dry/wet corrosion cycles.[12,13] In the case of Ni-bearing steel, cross-sectional observation of the rust using EPMA showed that Ni was uniformly distributed over the entire rust layer. Figure 4 shows the results from XPS analysis of the rust layer. Compared to reference compounds Ni, NiO, and Ni_2O_3, the Ni $2P_{3/2}$ peak from the Ni-bearing steel is similar to that of NiO. This result indicates that Ni was incorporated into the iron oxide as a bivalent state.

Figure 5 shows the spectra for the rust on the Co-bearing steel (dots in the Figure) and the reference spectra, after the peak strength of the Co Lα X-ray was normalized to 1.0. When the peak strengths are compared to Co Lβ X-ray peaks, the spectrum of the Co-bearing steel is similar to that of CoOOH. Furthermore, when peak positions of Co reference Co compounds.

Lα X-ray are compared, results for Co-bearing steel are

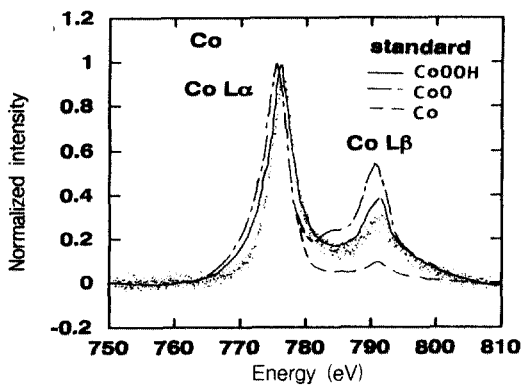

Fig. 5. XPS spectra for the rust of a Co-bearing steel and reference Co Compounds

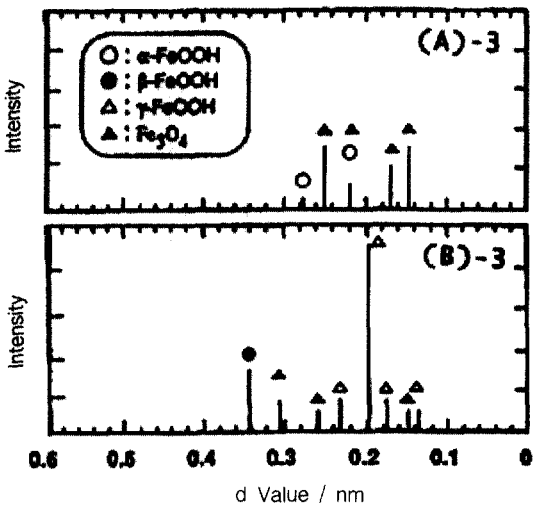

Fig. 6. Transmission electron diffraction of (A) Ni- and (B) Co-bearing steels. Selected areas for the diffraction corresponded to those of Ni- and Co-enrichment.

similar to those of CoOOH. This indicates that Co was incorporated into FeOOH as a trivalent state.

From the X-ray diffraction analysis, no significant increase in the amount on Fe_3O_4 was detected by the addition of Ni: the relative amount of Fe_3O_4 a few mass percentage. This result indicates that Ni was mainly included in an oxide that could not be detected by X-ray diffraction. More detailed examination was carried out by TEM. The rust was collected from the Ni-bearing steel, and the Ni-rich portion was selected using EDXS analysis (Figure. 6A)-1). Figure. 6(A)-2 shows the electron diffraction pattern, which indicated the selected portion has the structure Fe_3O_4 or a kind of spenels. It was also found that the amount of FeOOH was small, and no other structure could be detected. These results were confirmed by observation of several specimens. Thus, Ni is usually included in the spinel-structured oxide similar to Fe_3O_4, which is difficult to be differentiated from Fe_3O_4 using XRD. By XPS analysis it is also established that Ni was present in the oxide mainly in a bivalent state, indicating that Ni replaces Fe(II) in the spinel structure. Cross sectional observation of the rust using EPMA indicated that the Co was uniformly distributed all over the rust layer in Co-bearing steel. X-ray spectra was determined by means of EPMA for the rust of Co-bearing steels. The X-ray peak characteristic of Co was compared with those reference spectra of compounds metallic Co, CoO, CoOOH.

3.3.2 Effect of Al addition

A steel bearing 0.8 mass % Al showed smaller mass loss in wet/dry cycle test than that of carbon steel.[14] The ratio of corrosion loss of carbon steel to 0.8 % Al steel

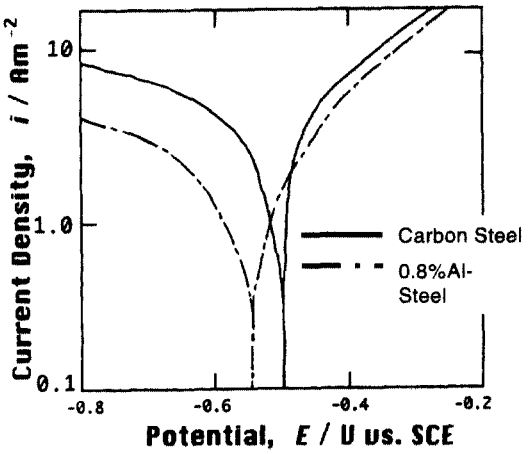

Fig. 7. Polarization curves for an Al-bearing steel obtained after the treatment of 8 cycles of wet/dry corrosion test.

increased with time and it reaches 75 % after 20 cycles. Polarization curves for a carbon steel and 0.8% Al-steel are shown Figure. 7. Both of the sample had been treated 8 cycles in wet/dry corrosion cycle test before polarization measurements.

After 20 cycles of corrosion test, EPMA cross sectional analyses showed the enrichment of Al in the inner layer of rust. By transmission electron diffraction of Al-enriched potion of rust has proven the formation of a spinel, suggesting the formation of $FeAl_2O_4$ similarly to the case of the Ni-bearing steel..

Al addition was effective in suppressing cathodic reaction but was not in anodic branch. XRD analysis proved that ratio of β-FeOOH is less in the rust of the Al-bearing steel. Since β-FeOOH is the most readily reduced to Fe_3O_4, its suppressed production in turn will result in the decrease in cathodic current. One reason for the increased β-FeOOH is due to the fact that the external layer is easily removed in the process of pure water rinse. The readiness to form $FeAl_2O_4$ spinel may inhibit the reoxidation to ferric state in dry process.

3.3.3 Effect of W addition

A steel bearing 1 mass % W showed smaller mass loss in wet/dry cycle test than that of carbon steel.[15] The ratio of corrosion loss of carbon steel to 1 % W steel increased with time and it reaches 70 % after 20 cycles. Polarization curves in 0.1 % NaCl solutions are shown in Figure. 8. Curves A and B show those for W-bearing and plain carbon steel in a 0.1 %NaCl solution, respectively. Curve C represents that for plain carbon steel in a 0.1 % NaCl-0.05M Na_2WO_4 solution. Obviously the effect of alloying was minor (Curves A and B) except for the fact that anodic branch current is suppressed for W-bearing steel. In

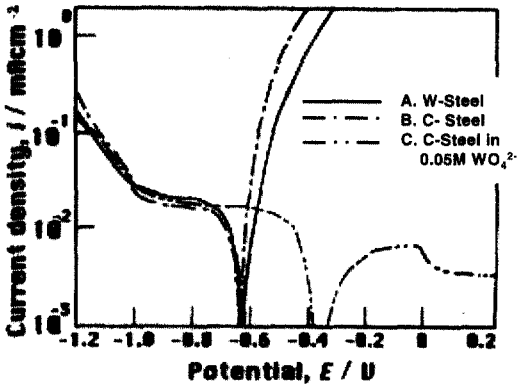

Fig. 8. Polarization curves for W-bearing steel in NaCl solution and 0.05 M WO_4^{2-} - NaCl solution.

Na_2WO_4 containing solution (Curve C), however, anodic inhibition is remarkable, despite its fact that its effect on cathodic reaction is very negligible.

Instrumental analyses were carried out for W-bearing steel after 20 cycles of the wet/dry corrosion test. By EPMA mapping of a cross-section it has bee proven that W is enriched in the inner portion of rust layer. XPS spectra of the rust of W-bearing steel showed two peaks of W, ie, $W_{4f5/2}$ and $W_{4f7/2}$, from which the latter is used for identification with reference to standard samples of WO_2, WO_3, $WOCl_4$ and H_2WO_4. The maximum peak of W in the rust is located the closest to that of H_2WO_4, indicating that W exists in its hexavalent state (WO_4^{-2}).

Both electrochemical data and instrumental analyses suggest that the effect of W addition in the stabilization of rust exists in the fact that W functions as an anodic inhibitor in the form of WO_4^{-2}.

3.4.4 E-pH diagram for Fe-M systems

It has been demonstrated that the alloying elements in steel is incorporated into rust either forming double oxide like spinel, or substituting Fe(II) or Fe(II) ion of FeOOH or Fe_3O_4 or forming iron salt in the form of oxy-anions. The incorporation may take the form of adsorption or double oxide formation. In the corrosion process of weathering steels it is recognized that stabilization of rust proceeds through the coprecipitation or sorption of minor elements to ferric hydroxide. Since the data are scarce for the stability estimation of double oxide formation in aqueous media, high temperature thermodynamical data were used for the evaluation of coprecipitation tendency. Figure 9 to 12 are E-pH diagrams for Fe-X-H_2O systems where X are alloying elements for weathering steels.[16-18]

4. Conclusion

Low-alloy weathering show poor performance in en

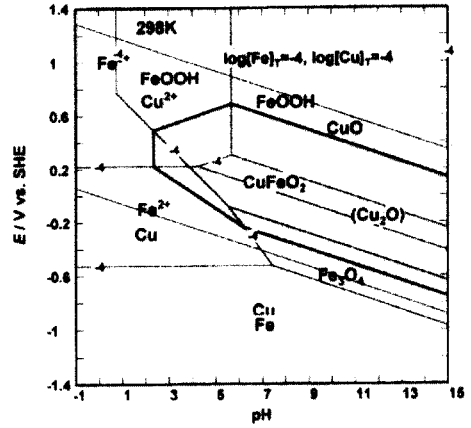

Fig. 9. E-pH diagram for Fe-Cu system.

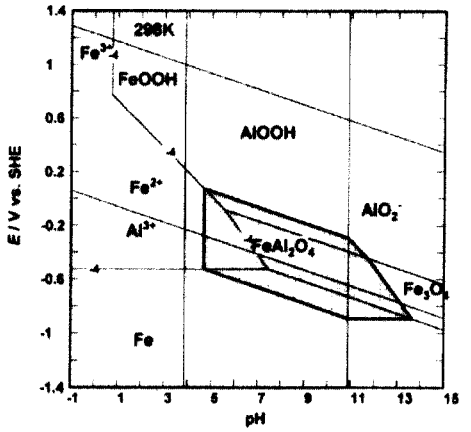

Fig. 11. E-pH diagram for Fe-Al system.

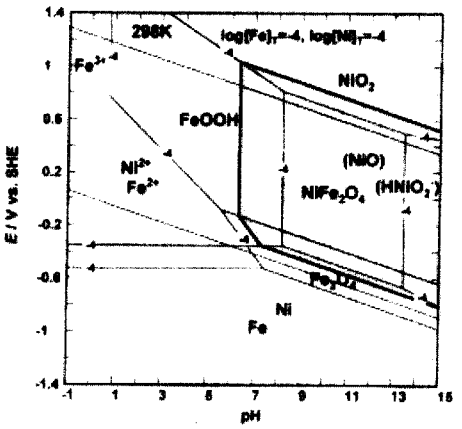

Fig. 10. E-pH diagram for Fe-Ni system.

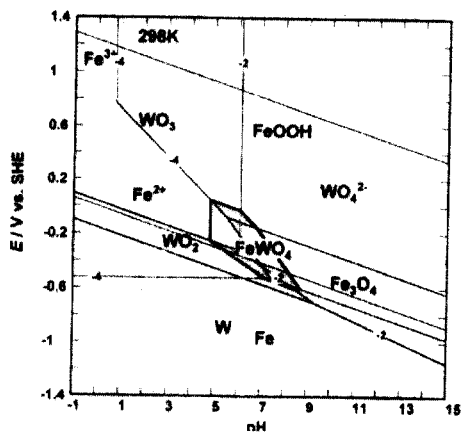

Fig. 12. E-pH diagram for Fe-W system.

vironments where airborne salinity is high. Recent research on rust and weathering steels has been focused on the rusting mechanism in the presence of chloride and development of new steels and coatings that are resistant in marine/coastal environments. The paper focuses on 1) tolerable limit of airborne salinity level for the use of uncoated weathering steels in infrastructure, 2) thermochemical aspect of rusting in chloride environments, 3) crystal structure of iron rust in high salinity, 4) electrochemical reaction of rust and its catalytic properties in chloride media, 5) protective nature of rust of weathering steels.

References

1. Report of weathering steel for bridge (XVIII) Public Works Research Institute, *Ministry of Construction of Japan* 1 (1993).
2. U. S. Department of Transportation, Federal Highway Administration, Technical Advisory T5140.22 *"Uncoated Weathering Steel Structures,"* Oct. 3 (1989).
3. T. Nishimura, K. Kurosawa, and T. Kodama, *196th Meeting of the Electrochemical Society ECS,* 458 (1999).
4. T. Nishimura, H. Katayama, K. Noda, and T. Kodama, *Zairyo-to-Kankyo* **49,** 45 (2000).
5. U.R. Evans, *Nature*, **206**, 980 (1965).
6. I. Matsushima and T. Ueno, *Boshoku Gijutsu*, **17**, 458 (1968) .
7. I. Suzuki, N. Masuko, and Y. Hisamatsu, *Corros. Sci.*, **19**, 521 (1979).
8. H.Okada, Y. Hosoi, K.Yukawa, and H. Naitoh, *Tetsu to Hagane*: **55**, 355 (1969).
9. H. Miyuki, M. Yamashita, M. Fujiwara, and T. Misawa, *Zairyo to Kankyo*, **47**, 186 (1998).
10. M. Yamashita, H. Miyuki, H. Nagano, and T. Misawa, *Tetsu to Hagane*, **83**, 448 (1996).
11. C.P. Larrabee, *Corrosion*, **15**, 526 (1959).
12. T. Nishimura, H. Katayama, K. Noda, and T. Kodama, *Corros. Sci.* **42**, 1611 (2000).
13. T. Nishimura, H. Katayama, K. Noda, and T. Kodama, *Tetsu-to-Hagane,* **86**, 111 (2000).
14. T.Nishimura, A.Tahara, and T. Kodama, *Materials Trans.* **42**, 478 (2001).
15. T. Nishimura, K. Noda, and T. Kodama, *Zairyo-to-Kankyo* **49**, 734 (2000).
16. T. Kodama, *Proc. Asian-Pac. Corros. Control Conf. 8th* 98 (1993).
17. T. Tahara and T. Kodama, *Proceeding of JSCE* 33 (1998).